

Emerging coding methods for computational imaging

Kai Wu,^a Yuanfenghe Qu,^b Ruozhang Wang,^c Hao Li,^d Xinrui Ying,^e Pengyu Tian,^f Xilai Li,^g Zongliang Wu,^a and Xin Yuan^{a,*}

^aResearch Center for Industries of the Future and Department of Artificial Intelligence, School of Engineering, Westlake University, Hangzhou, China

^bSchool of Computer Science and Technology, Xidian University, Xi'an, China

^cFaculty of Information Engineering and Artificial Intelligence, Lanzhou University of Finance and Economics, Lanzhou, China

^dSchool of Mathematics and Computer Science, Nanchang University, Nanchang, China

^eFaculty of Engineering, University of Bristol, Bristol, United Kingdom

^fKey Laboratory of Intelligent Perception and Image Understanding of Ministry of Education, School of Artificial Intelligence, Xidian University, Xi'an, China

^gGuangdong-Hong Kong-Macao Joint Laboratory for Intelligent Micro-Nano Optoelectronic Technology, School of Physics and Optoelectronic Engineering, Foshan University, Foshan, China

Abstract. Computational imaging employs the joint design of optical modulation and reconstruction algorithms, overcoming the inherent physical limitations of conventional imaging. From the perspective of information transmission, computational imaging sequentially applies optical encoding, indirect measurement, and computational decoding to capture the desired information. This paradigm demonstrates superiority over conventional imaging in terms of information capacity, information acquisition efficiency, information dimensions, and information acquisition functionality. Optical encoding plays a pivotal role and can be implemented across multiple dimensions of light at various positions along the optical path. This mini-review surveys emerging encoding methods for computational imaging driven by optical element parameter optimization tools, micro-nano manufacturing, and non-classical properties of light. Differentiable optics and end-to-end optimization can model complex physical processes and further strengthen the integration of optical encoding and computational decoding. Advances in material science and micro-nano fabrication give rise to compact, high-performance imaging systems and propel the practical implementation of diverse, bio-inspired imaging. In addition, quantum properties and orbital angular momentum create new possibilities for encoding methods that perform better in specific conditions. The research in these areas represents the latest advances in computational imaging encoding methods and demonstrates the potential for rapid development in the future.

Keywords: computational imaging; optical encoding; differentiable optics; micro-nano optics; non-classical light.

Received Jul. 25, 2025; revised manuscript received Aug. 28, 2025; accepted Sep. 29, 2025; published online Nov. 10, 2025.

© The Authors. Published by Chinese Laser Press under a Creative Commons Attribution 4.0 International License. Distribution or reproduction of this work in whole or in part requires full attribution of the original publication, including its DOI.

[DOI: [10.3788/AI.2025.20004](https://doi.org/10.3788/AI.2025.20004)]

1. Introduction

Light has multiple inherent properties, including amplitude, phase, wavelength, polarization, spatial position, and propagation direction, making it a versatile carrier of information^[1]. Photomorphogenesis reveals that photoreceptors in plants can

respond to the light spectrum to regulate growth patterns. Similarly, the visual system of animals can perceive multiple color channels and polarization patterns of light for object recognition, navigation, and communication. Throughout history, humans have employed light-sensing and imaging technologies to measure and estimate various physical properties of the environment, ranging from microcosms to astronomy, leading to numerous scientific discoveries. In recent decades, the imaging

*Address all correspondence to Xin Yuan, xyuan@westlake.edu.cn

paradigm that combines optical encoding and computational decoding has opened new ways for the visual perception of the physical world.

Conventional imaging relies on object–image spatial mapping and intensity-based direct measurement modes, resulting in the loss of multidimensional optical information, and performance improvement is limited by the diffraction limit, optical aberrations, noise, etc. Driven by advancements in optics, image processing, and information theory, along with growing application demands, researchers are increasingly focusing on the joint design of optical modulation and reconstruction algorithms. This paradigm, known as computational imaging, has been shown to improve imaging performance, enable the acquisition of multidimensional optical information, and unlock groundbreaking functionalities^[2].

From the perspective of information transmission, computational imaging (Fig. 1) introduces the idea of information encoding within the imaging pipeline, sequentially applying optical encoding, indirect measurement, and computational decoding to the desired information^[3]. Optical encoding represents the physical process in which light propagates from the source to the detector. This process also involves the scene, lenses, modulators, and other optoelectronic devices, which play roles in controlling the properties of light. Encoding implies that the detector measurement process is an intermediate step rather than the final one. Additionally, mathematical modeling of the optical encoding and reconstruction algorithms enables the decoding of a scene’s property information from the intensity measurements. Compared with the direct mechanism of

conventional imaging, this transformation increases information capacity, improves information acquisition efficiency, expands the information dimensions, and provides groundbreaking information acquisition functionalities that were previously unattainable^[2,3]. In recent years, advances in micro-nano optics, artificial intelligence (AI), and differentiable optics modeling have led to the emergence of various computational imaging systems. However, it is still highly demanded to develop new coding methods in terms of the precise modeling of physical processes, implementation of joint design concepts, and the requirements of hardware, computational complexity, and imaging accuracy.

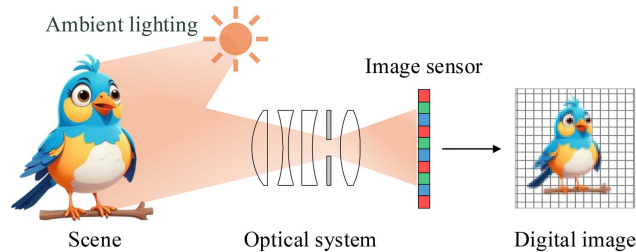
This paper presents an overview of the foundations and emerging research in computational imaging encoding methods, with the aim of providing a systematic understanding and inspiring further innovation in this field. First, we review concepts, realizations, motivations, and encoding–decoding frameworks of computational imaging in Sec. 2.1. Then, we briefly discuss the theoretical aspects of optical encoding for computational imaging and summarize the encoding methods based on encoding occurrence planes in Sec. 2.2. Finally, Sec. 3 presents a detailed discussion of several representative and promising emerging encoding methods, including their principles and applications.

2. Computational Imaging

2.1. Concepts, Realizations, and Motivations

The development of imaging technology has a remarkably long and illustrious history (Fig. 2), which is divided into five distinct periods: the ancient era of discovering the fundamental imaging

(a) Conventional imaging



(b) Computational optical imaging

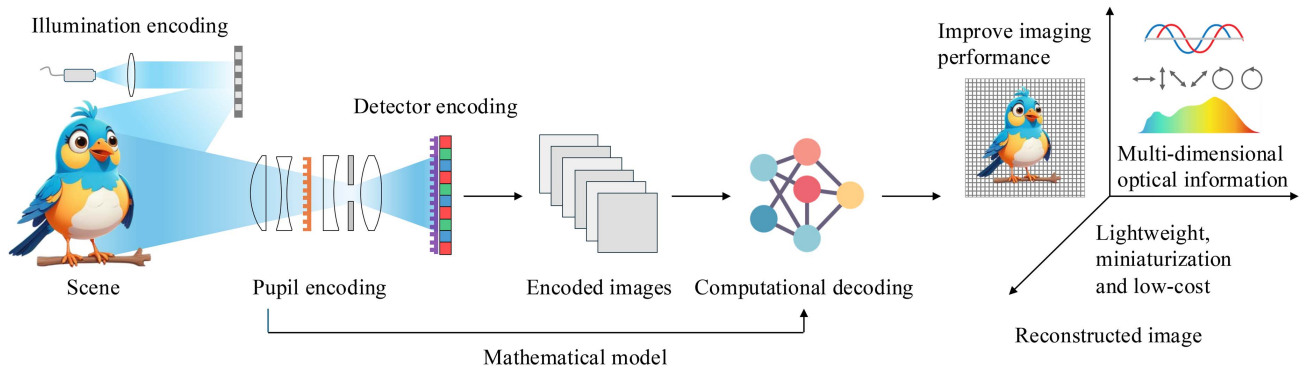


Fig. 1 Schematic diagrams of (a) conventional imaging and (b) computational optical imaging architectures. In computational imaging, encoding can be implemented in the illumination or pupil plane or embedded in the sensor itself. The detector measurement process is an intermediate step. Reconstruction algorithms then decode the scene’s property information from the encoded images. Compared with conventional imaging, computational imaging offers numerous advantages.

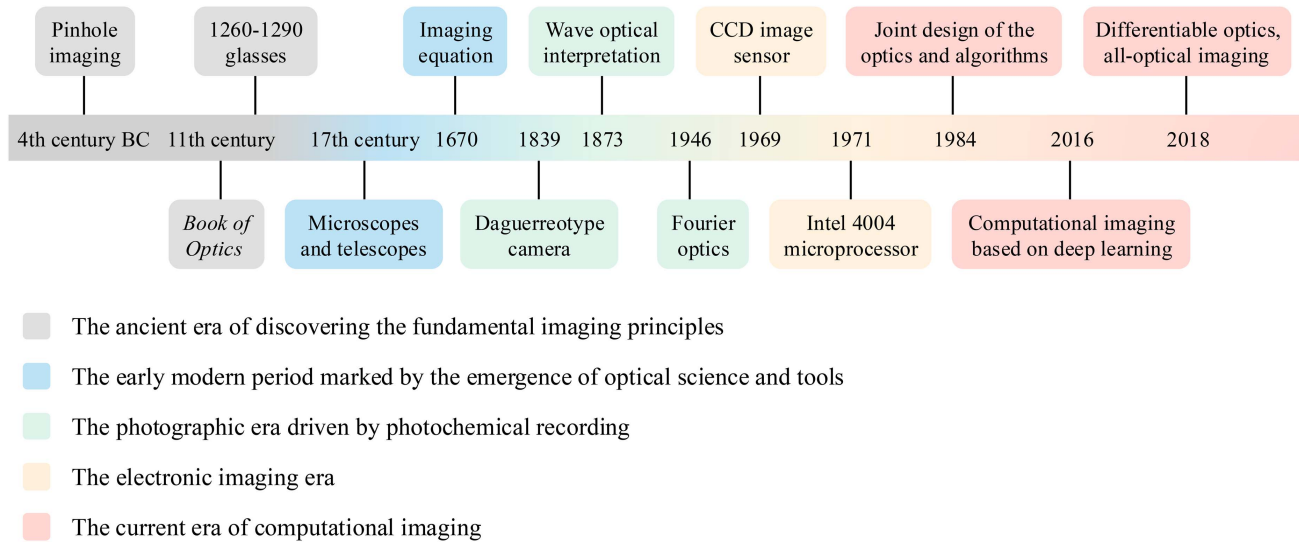


Fig. 2 A brief history of imaging technology.

principles, the early modern period marked by the emergence of optical science and tools such as microscopes and telescopes, the photographic era driven by photochemical recording, the electronic imaging era characterized by digital technology, and finally the current era of computational imaging that we are living in^[2].

Conventional photoelectric imaging uses optical lenses to focus light onto photodetectors, which convert the optical signals into electrical signals that are subsequently processed to generate images. Though characterized by efficiency, intuitive design, and straightforward implementation, its performance is fundamentally limited by physical laws, including the diffraction limit, optical aberrations, and noise. When light passes through a finite aperture, diffraction occurs, causing the image of a point in the object to appear as an Airy disk. The size of the Airy disk is inversely proportional to the aperture diameter, and the overlap of Airy disks results in a diffraction-limited spatial resolution. The discrete sampling by digital image sensors with non-zero pixels also limits the spatial resolution. Resolution, together with the field-of-view (FoV), determines the space-bandwidth product (SBP), which quantitatively characterizes the amount of detail that an imaging system can capture and serves as a key metric for evaluating the system's information-carrying capacity. In practical optical systems, the paraxial approximation is not strictly satisfied. Consequently, light rays originating from a point on the object may fail to converge precisely to a point on the image plane, leading to optical aberrations. Moreover, various types of noise may be introduced during the image acquisition process. The discrete nature of photons gives rise to statistical fluctuations, resulting in shot noise. The signal processing circuit of the image sensor can introduce dark current, readout noise, quantization noise, etc. Stray light can also degrade the signal-to-noise ratio (SNR). Besides, conventional imaging primarily relies on directly captured intensity images, which can limit its effectiveness in scenes involving multidimensional optical information.

In addition to the designs of complex optical lenses and high-performance sensors, researchers have also utilized image processing such as image denoising and super-resolution to meet application requirements. Image processing typically

operates on pixel data and is designed independently of optical systems.

Against the backdrop of flourishing optical designs and image processing methods yet lacking integration, Cathey *et al.* innovatively considered the joint design of forward measurement models and reconstruction algorithms to achieve improved resolution^[4]. This joint optical-computational approach represented a new imaging paradigm and was termed computational imaging subsequently^[2,5]. It should be emphasized that the reconstruction algorithms are designed in accordance with the mathematical model of the measurement process, unlike image processing, which is agnostic to the optical modulation process.

Conventionally, optical imaging focuses on the design and use of lenses, but advancements in photoelectric technology have expanded its scope. In the 19th century, Kerr and Pockels discovered the electro-optical phenomenon that optical properties of materials can be changed with external electric and strain fields, giving rise to a range of modern optical elements for controlling light. Since the early 1980s, significant advancements in micro-nano photonics, metamaterials, micro-electro-mechanical systems (MEMS), and related fields have enabled the development of light modulation devices featuring energy efficiency, compact sizes, broad bandwidths, and high speed. Currently, diverse light modulation devices and methods play a crucial role in optical imaging, quantum optics, integrated optics, and optical computing.

Computational imaging leverages modulation devices to control the distribution of light across multiple dimensions (Table 1). Key devices include metasurfaces^[6,7], digital micromirror devices (DMDs)^[8], liquid-crystal spatial light modulators (LC-SLMs)^[9], diffractive optical elements (DOEs)^[10,11], deformable mirrors^[12], color filter arrays (CFAs)^[13], polarizers^[14], film masks^[15,16], prisms, beam splitters, lenses, and mirrors. Flexible and precise optical modulation enables the transmission of light field information to bypass the physical limitations of light propagation and detector measurement. Specifically, this can be achieved through the compression of light field information, by sacrificing information in other dimensions or by employing other means. Generally, light modulation also involves the photoelectric conversion by the detector. In this context, the

Table 1 Light Modulation Devices Control the Distribution of Light Across Multiple Dimensions.

Device	Intensity	Phase	Spectrum	Polarization	Direction
Metasurface	✓	✓	✓	✓	✓
DMD	✓	✓ ^a	–	–	✓
LC-SLM	✓ ^a	✓	–	✓ ^a	✓
DOE	✓	✓	✓ ^a	–	✓
Deformable mirror	–	✓	–	–	✓
CFA	–	–	✓	–	–
Polarizer	–	–	–	✓	–
Film mask	✓	✓ ^a	–	–	✓
Prism	–	–	✓	–	✓
Beam splitter	✓	–	✓ ^a	✓ ^a	✓
Lens/Mirror	–	✓	–	–	✓

^aindicates implementation-dependent capability.

mathematical model of optical modulation can be represented as a mapping from high-dimensional signals to intensity measurements^[17,18]. These high-dimensional signals, representing multi-dimensional properties of the light field scene, are retrieved from measurements using reconstruction algorithms and stored as data cubes. Intensity measurements can be captured in a single snapshot, as in snapshot compressive imaging (SCI)^[19], or in multiple snapshots, as in ptychography^[20], which captures multiple images with scanning in a single measurement.

In computational imaging, recovering high-dimensional signals from intensity measurements is essentially a nonlinear ill-posed inverse problem. This is mainly due to the fact that the dimension of the solution space is much larger than that of the measurement space, the non-convex relationship between the high-dimensional signals and the measurements, as well as the influence of noise^[21]. Reconstruction algorithms are briefly summarized in Fig. 3. Conventionally, this ill-posed problem is

addressed using model-based optimization algorithms. The objective function, comprising a data fidelity term and a regularization term, is minimized using gradient descent, the alternating direction method of multipliers (ADMMs)^[22], or other methods. Regularization terms, such as total variation (TV)^[23] or sparsity^[24], help stabilize the solution space, suppress noise, and improve the quality of reconstruction results. Recent advances in deep learning have further revolutionized reconstruction algorithms. Deep neural networks (DNNs) can learn end-to-end mapping from measurement data to high-dimensional signals^[25]. Generative models, including the generative adversarial network (GAN) and diffusion models, have also been introduced in the reconstruction process. These models can learn complex priors from datasets and improve the quality of reconstruction results^[26]. In addition, physics-based deep learning bridges the gap between model-based and data-driven methods, merging the advantages of these two kinds of methods^[27]. Two frameworks,

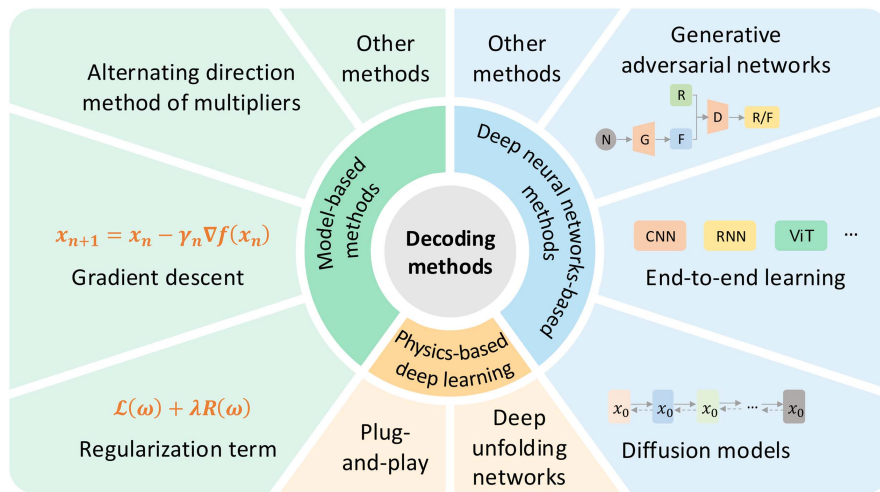


Fig. 3 A brief summary of the reconstruction algorithms for computational imaging, including the model-based methods (top left), deep-neural-network-based methods (top right), and physics-based deep learning methods (bottom).

deep unfolding networks^[28] and the plug-and-play (PnP) framework^[29], have put this concept into practice.

Computational imaging utilizes algorithms to share the hardware burden and overcome physical limitations, thereby surpassing the performance of conventional imaging and enabling imaging functionalities that were previously unattainable^[2]. As shown in Fig. 4, the former is reflected in super-resolution imaging, SNR improvement, high dynamic range (HDR) imaging, depth of field (DoF) extension, motion deblurring, large FoV imaging, spectral imaging, polarization imaging, computational ultrafast imaging, adaptive optical imaging, and minimalist optical systems^[3]. Computational imaging can bypass physical limitations to provide a feasible solution for these performance improvements or demonstrate advantages over conventional implementations in terms of speed, size, weight, power, and cost. The examples of the latter include light field imaging^[30], three-dimensional (3D) surface imaging^[31], quantitative phase imaging (QPI)^[32], scattered light imaging^[33,34], single-pixel imaging (SPI)^[35], 3D volumetric imaging^[36–40], and quantum imaging^[41].

2.2. Optical Encoding

Researchers have used information theory to analyze and evaluate imaging systems for a long time. In the information-theoretic visual communication channel model, the image gathering system, as a transmitter, encodes the radiation field within the FoV into a signal to be transmitted, while the image restoration

process, as a receiver, decodes the received signal^[42]. Specifically, the encoding process involves actively or passively illuminating the scene, as well as the propagation of electromagnetic waves from the scene to the detector. Some literature also includes the photoelectric conversion of the detector within the scope of encoding^[17]. The inherent factors of optical and optoelectronic devices limit the performance of visual communication channels. The utilization of encoding and decoding methods is expected to achieve optimal scene reproduction under specified conditions and performance criteria.

The encoding process involves a series of optical and optoelectronic elements, each corresponding to a sub-process of optical modulation and being modeled as a sub-mapping. For example, coherent light-emitting diode (LED) illumination induces a wave-vector-dependent shift in the Fourier spectrum of the object's complex amplitude, the phase transformation characteristic of a converging lens enables the implementation of a two-dimensional Fourier transform, and the signal modulation function of a mask can be represented by element-wise matrix multiplication. These sub-mappings are integrated to form the overall mapping from high-dimensional scene signals to intensity measurements of the detector:

$$y = S \circ f_n \circ f_{n-1} \circ \dots \circ f_1(x), \tag{1}$$

where S denotes the sensing process of the detector. It should be noted that manufacturing imperfections of the elements and process noise can introduce uncertainties into the mapping model,

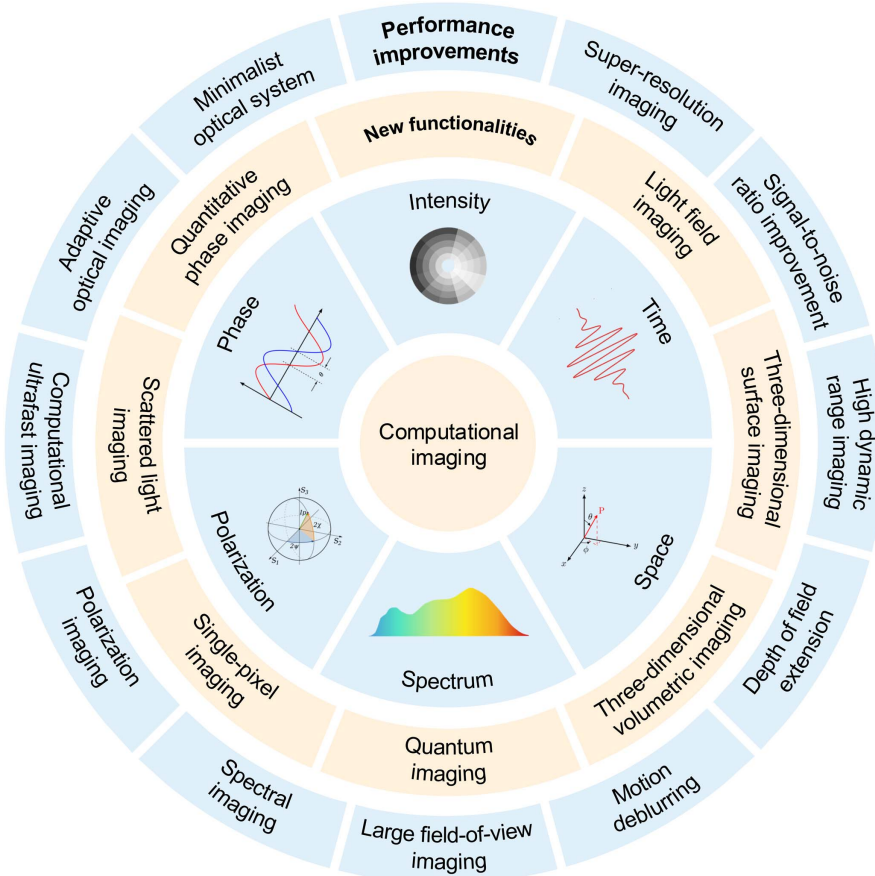


Fig. 4 A brief summary of the computational imaging applications.

which are commonly difficult to represent explicitly in mathematical terms.

Encoding sub-processes can be introduced at various positions along the optical path, including the light source, pupil, detector, or combinations thereof^[1]. Encoding can be designed to modulate specific light field dimensions or their combinations. Table 2 provides a summary of optical encoding methods categorized based on encoding occurrence planes. In addition, when propagating through scattering media such as emulsions, multimode fibers, and biological tissues, light is extensively scattered, severely disrupting the transmission of optical information. In conventional imaging, scattering is viewed as a

source of interference that degrades imaging performance. By contrast, in computational imaging, scattering media is considered to be an encoder that transforms the input optical field into a complex speckle pattern. Deep learning or model-based algorithms can decode the optical field information from these complex speckle patterns^[43]. Wavefront shaping methods can precisely control the scattered light field by measuring the transmission matrix of the scattering media or achieve refocusing of the scattered light via phase conjugation^[44,45]. These research advancements hold significant potential for imaging in complex media and expand the encoding methods for computational imaging.

Table 2 Summary of Different Computational Imaging Coding Methods and Implementations.

Class of Method	Example
Illumination coding	
Structured light pattern ^[31,46-48] and implementation	Speckle pattern, binary code, gray code, phase shifting, gray code with phase shift, strip indexing, grid indexing, color code, and phase unwrapping
Illumination scanning	Beam interference ^[49] , multifocal exciting light ^[50] , optical waveguide array evanescent field ^[51] , spatial light modulator (SLM) ^[52] , DOE ^[53] , DMD ^[54] , and metasurface-driven ^[55]
Light detection and ranging (Lidar)	Illumination array ^[56] , adaptive illumination ^[57,58] , wavelength and angular multiplexing ^[59-62] , multiplexed source coding ^[63] , wavelength scanning ^[64] , and rapid laser beam scanning ^[65-67]
Coded exposure (flutter shutter)	Direct time-of-flight (ToF) ^[68] , amplitude-modulated continuous wave (AMCW) ^[69] , frequency-modulated continuous wave (FMCW) ^[70] , stepped frequency continuous wave (SFCW) ^[71] , multi-spectral ^[72] , spectrally scanning ^[73] , and ultrafast and high-FoV metasurface scanning ^[74]
Light interference	Temporal coding ^[75,76] , per-pixel coding ^[77,78] , and spatial-temporal coding ^[79]
Pupil coding	
Metasurface-based	Time-domain optical coherence tomography (OCT) ^[80] , spectral-domain OCT ^[81] , swept-source OCT ^[82] , in-line holography ^[83] , and off-axis holography ^[84]
Camera array	Achromatic imaging ^[85,86] , hyperspectral imaging ^[87] , polarization imaging ^[88,89] , snapshot Mueller matrix imaging ^[90] , snapshot full-Stokes imaging ^[91] , point spread function (PSF) engineering ^[92] , synthetic aperture ^[93] , and snapshot multidimensional imaging ^[94]
Aperture scanning	Wide-field high-resolution imaging ^[95] , multi-focal length ^[96] , multiple spectra ^[97] , and synthetic aperture ^[98]
Coded aperture	Wide-field high-resolution imaging ^[99] , multiple spectra ^[100] , and synthetic aperture ^[101]
Minimalist optical system	Random coded aperture ^[102] , uniformly redundant array ^[103] , modified uniformly redundant array ^[104] , Fresnel zone aperture ^[105] , time-multiplexing ^[106] , and snapshot spectral imaging ^[107]
Adaptive optics system	Single-lens imaging ^[108] , freeform optics ^[109] , lensless imaging ^[110] , and end-to-end compact design ^[111]
Microlens array	Shack-Hartmann wavefront sensor ^[112] , curvature wavefront sensor ^[113] , pyramid wavefront sensor ^[114] , diffusive plates ^[115] , and indirect wavefront sensing ^[116]
Single-pixel detector	Deformable mirror correction ^[117] , liquid crystal SLM correction ^[118] , and deformable phase plate correction ^[119]
	Light field camera ^[120] , snapshot 3D and polarization ^[121] , and snapshot hyperspectrum ^[122]
	Single-pixel imaging ^[123] , ghost imaging ^[124] , and single-photon imaging ^[125]
Detector coding	
Super-resolution detector	Micro-scanning ^[126] , focal plane coding mask ^[127] , and multi-aperture camera sub-pixel shifting ^[128]
Non-uniform detector	Single-pixel camera array ^[129] , synthetic aperture radar ^[130] , and shape-awareness ^[131]
Curved surface detector	Digital X-ray detector ^[132] , hemispherical nanowire array retina ^[133] , curvy and shape-adaptive detector ^[134] , and biomimetic multispectral curved compound eye camera ^[135]
Multidimensional detector	Dispersion-assisted high-dimensional photodetector ^[136] , broadband hyperspectral image sensor ^[137] , and spectrometer with electrochromic modulation ^[138]

Before the advent of digital image sensors, image processing was primarily performed using analog circuits, optical devices, or chemical methods. The digital image sensor is a bridge of optical and digital world, propelling the development of image processing and further giving rise to computational imaging. Conventional optical devices are bulky and have limited modulation parameter space, thereby restricting the development of optical encoding theory and application. There is an urgent need for light modulation devices that allow the free design of encoding methods.

In recent years, advances in micro-nano materials and fabrication techniques, together with deep-learning-driven inverse design of optical systems, have been transforming optical engineering^[139,140]. For example, diffractive optical processors based on DOEs and metasurfaces composed of subwavelength unit cells enable precise and customized modulation of optical fields, thereby facilitating the development of computational imaging, optical information processing, photonic computing, and other applications^[86,87,89,141–143]. These micro-nano optical devices promise to serve as another bridge between the optical and digital worlds, promoting the deployment of encoding models in optical systems.

Encoding is essentially a mapping process that is realized through computation. Complex computations commonly enhance the encoding capability. As shown in Fig. 5, diffractive deep neural networks (D²NNs) and metamaterials have an extensive parameter space and are capable of performing complex computations. Complex encoding models can be deployed in optical networks, enhancing imaging performance. For example, Shi *et al.* employed diffractive optical network encoding and electronic neural network decoding for high-dynamic all-focus imaging^[146]. Some research demonstrates all-optical imaging with diffractive encoding and decoding, where the diffractive decoder can perform instantaneous image reconstruction with performance surpassing that of DNN-based digital decoders^[147,148]. These advances further imply that computation is introduced not only in the reconstruction process, but also during the image-gathering process. Consequently, the encoding–decoding paradigm has been evolving from a conceptual representation to practical implementation within computational imaging systems. In this context, we can seek inspiration from information theory and computer science to form a universal and scalable imaging framework for further advancing the development of computational imaging.

Optical encoding plays a pivotal role in computational imaging. We survey the recent literature on computational imaging and note that the emerging encoding methods are primarily

driven by optical element parameter optimization tools, micro-nano manufacturing, and non-classical properties of light. The research in these areas still demonstrates great potential for rapid advancement in the future.

3. Emerging Coding Methods

3.1. Differentiable Optics Modeling, End-to-End Optimization, and Inverse Design

3.1.1. Concepts and principles

The core of differentiable optics modeling lies in describing an optical system using mathematical models and converting its physical parameters into differentiable tensors or variables^[17,149,150]. In this way, the entire optical process can be formulated as a continuous, differentiable computational graph, thereby supporting gradient-based optimization algorithms. Differentiable optics modeling involves the physical propagation of light and its interaction with optical elements. Given the input field, the Rayleigh–Sommerfeld diffraction formulas can yield the output field under certain physical conditions. In most cases, by employing the angular spectrum, Fresnel, or Fraunhofer diffraction approximations, one can obtain simpler forms of light propagation formulas^[18]. Optical element parameterization refers to the transformation of physical quantities, including those describing geometric shapes, optical properties, and systematic errors, into parameters that can be optimized via gradient descent. Examples include the focal length of a thin lens, Zernike polynomial coefficients describing wavefront aberrations, transmittance values at each position of a programmable aperture, phase modulation values of individual pixels on LC-SLMs, structured light encoding patterns, and parameters of noise probability distributions.

The joint design of optical encoding and computational decoding is the core concept of computational imaging. End-to-end optimization is an emerging research direction of the joint design concept, enabling the convergence of optical elements and algorithms. Specifically, in an image gathering system, each optical element is modeled as an optical layer with learnable parameters, forming a fully differentiable encoder composed of multiple layers:

$$\mathbf{y} = H_{\phi}\mathbf{x} + \omega, \quad (2)$$

where H_{ϕ} denotes the optical encoder, \mathbf{x} represents the high-dimensional scene signal, \mathbf{y} is the encoded measurement, and

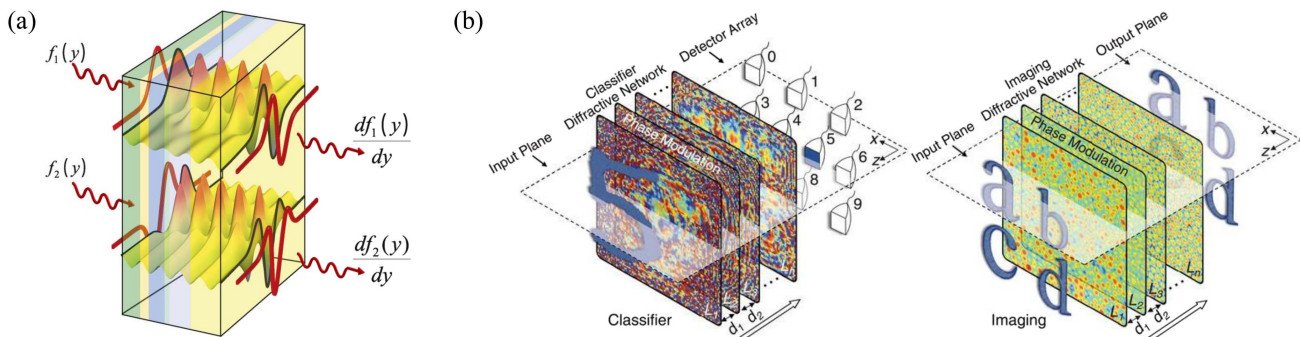


Fig. 5 (a) Wave-based metamaterial computing, reproduced with permission from AAAS^[144]. (b) Different types of D²NNs: classifier and imager, reproduced with permission from AAAS^[145].

ω represents the additive noise. H_ϕ involves light propagation, light modulation with optical elements $\phi = \{\phi^l\}_{l=1,2,\dots,n}$, and the sensing process of the detector. When employing a DNN as the decoder, the parameters of both the encoder and decoder can be optimized in an end-to-end manner using the backpropagation algorithm and datasets:

$$\{\theta^*, \phi^*\} = \arg \min_{\phi, \theta} \frac{1}{K} \sum_{k=1}^K \mathcal{L}[\mathcal{M}_\theta(H_\phi \mathbf{x}_k), \mathbf{d}_k] + \rho R_\rho(\phi) + \sigma R_\sigma(\theta), \quad (3)$$

where $\{\phi^*, \theta^*\}$ represents the optimal parameters of the encoder H_ϕ and the decoder \mathcal{M}_θ , respectively, $\{\mathbf{x}_k, \mathbf{d}_k\}_1^K$ denotes the training dataset, \mathcal{L} denotes the loss function, $R_\rho(\phi)$ and $R_\sigma(\theta)$ are the regularization functions that act in the parameters of the encoder and the decoder, respectively, and ρ and σ are the regularization parameters^[151,152].

Differentiable optics and end-to-end optimization can parameterize noise, errors, and manufacturing defects, model complex physical processes, and further strengthen the integration of optical encoding and computational decoding, promising to play a key role in advancing the development of computational imaging^[17].

As the functional complexity and design freedom of optical systems increase, researchers have introduced inverse design strategies to enhance optical modulation performance^[153]. Inverse design refers to starting from the desired imaging effect or task objective and inferring the required system parameters or structures by solving an optimization problem. When explicit solutions are difficult to obtain through forward design, optimization algorithms can automatically generate design solutions that meet the requirements. End-to-end optimization based on differentiable optics is an important implementation of inverse design. Evolutionary optimization is another class of numerical optimization methods for inverse design that emulates the behavior of biological populations and operates without relying on gradient information. Widely used evolutionary optimization methods include genetic algorithms, ant-colony optimization, and particle swarm optimization. For example, Zhu *et al.* leveraged a multi-social genetic algorithm to design the speckle patterns modulated by DMDs^[154].

3.1.2. Implementations and applications

After the simulation design based on differentiable optics or evolutionary optimization is completed, optical elements will be manufactured and assembled according to the learned parameters. Due to factors such as the manufacturing defect, there are often discrepancies or mismatches between simulated designs and actual optical fabrication. The response of the actual optical system can be characterized by measuring the point spread function (PSF) and other methods. By fine-tuning the decoder, that is, retraining the DNN weights using a small set of measurements from real scenes, the network performance can be optimized, thereby enhancing the system's robustness and fidelity in practical applications^[151]. For example, Zheng *et al.* proposed a novel method termed neural lithography to address the gap between design and fabrication in the field of computational optics^[155]. They built a physics-based neural network to serve as a differentiable digital twin model of the lithography system and trained it using a dataset collected experimentally. The effectiveness of the proposed method was verified through experiments

in designing and fabricating holographic optical elements (HOEs) and multilevel diffractive lenses (MDLs).

In recent years, the end-to-end optimization framework has garnered widespread attention and has been applied in numerous computational imaging tasks. For example, Jacome *et al.* used a set of regularization functions to improve the design of optical coding elements in the end-to-end optimization framework [Fig. 6(a)]^[152]. The proposed method was validated on a single-pixel camera and coded aperture snapshot spectral imager. Arya *et al.* embedded an iterative and non-approximated compressed sensing reconstruction algorithm into the end-to-end optimization pipeline to optimize the metasurface structures [Fig. 6(b)]^[156]. The experimental results in single-channel imaging and high-resolution 3D imaging demonstrate that the optimized metasurface achieves a significant improvement in performance compared to random scattering surfaces. Chen *et al.* parameterized defocusing and illumination amplitude variation in holographic imaging [Fig. 6(c)]^[157]. Seong *et al.* utilized the end-to-end framework to jointly optimize the binary phase filter (BPF) and the reconstruction algorithm for extended DoF microscopy [Fig. 6(d)]^[158]. Shao *et al.* proposed wavelength-multiplexed multimode extreme ultraviolet (EUV) reflection ptychography based on automatic differentiation (AD), demonstrating powerful capabilities of AD in handling complex physical processes and experimental uncertainties^[159]. The end-to-end optimization paradigm has also been applied to other kinds of optical elements and various applications, including HDR imaging, microscopic imaging, large FoV imaging, and time-of-flight (ToF)^[18].

However, due to the inherent characteristics of deep learning, end-to-end optimization frameworks face challenges in terms of generalization, interpretability, and robustness. The hardware implementation of the optimal encoding scheme obtained through training may be affected by manufacturing precision, noise, and system imperfections. Changing tasks or application scenarios may require retraining and reconfiguring the optical encoding scheme, which imposes high demands on hardware reconfigurability and results in low system update efficiency and high maintenance costs. New methods are required to tackle these challenges.

3.2. Coding with Advanced Materials and Devices

3.2.1. Integrated design

Recent research demonstrates the trend toward miniaturization and integration in optical systems. Advancements in materials science and micro-nano fabrication technologies have enabled optical modulation to eliminate the need for bulky, multi-element optical systems, favoring instead compact and integrated architectures.

Integrated and miniaturized structured light modulation techniques have garnered increasing attention, holding promise for new opportunities in fields such as imaging^[160]. For example, Lyu *et al.* utilized metasurface subwavelength structures to precisely control phase and dispersion, achieving high-density multi-wavelength dot array projection, which significantly enhances the resolution and accuracy of 3D imaging^[161]. Lin *et al.* attached a photonic integrated circuit (PIC) to a standard wide-field microscope to improve QPI^[162]. The PIC enables switchable illumination without mechanical movement and provides oblique illumination beams at precise angles, significantly reducing the phase noise. Nanophotonic approaches

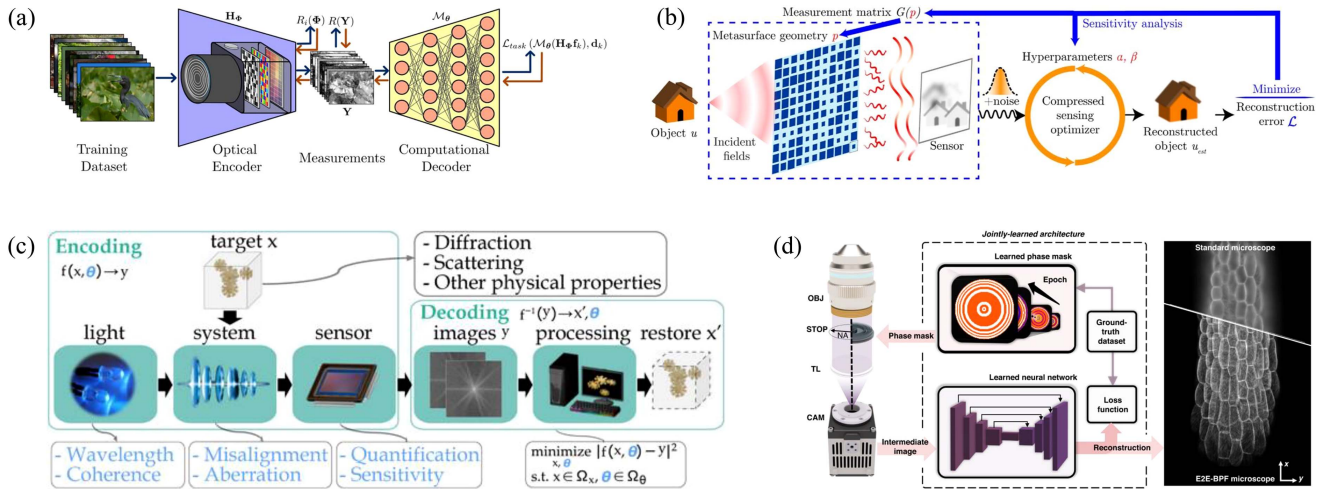


Fig. 6 End-to-end optimization for computational imaging. (a) End-to-end scheme where the optical encoder is optimized jointly with the computational decoder network, reproduced with permission from Optica Publishing Group^[152]. (b) A compressed sensing minimization problem is nested within the end-to-end optimization pipeline for a metasurface imaging system, reproduced with permission from ACS^[156]. (c) Realistic factors in a typical holography system that may affect the modeling. ∂H models and retrieves some of these parameters, reproduced with permission from John Wiley & Sons^[157]. (d) An axi-symmetric BPF and an image reconstruction network are jointly learned through the physics-informed neural network, reproduced with permission from Springer Nature^[158].

are advancing the miniaturization and high-performance of LiDAR systems through technologies such as PICs, optical phased antenna arrays, and metasurface-based planar optical devices^[72,163].

With the advancement of semiconductor manufacturing technology, as shown in Fig. 7, many functionalities that conventionally relied on complex optical systems can now be directly implemented at the chip level of image sensors. To a certain extent, new sensors are on the verge of emerging. Fan *et al.* designed a thin-film structure with spatial dispersion (non-local effects) that can encode different polarization and spectral information into the wave vector space^[136]. The optical field information is then decoded using a deep residual network (ResNet). This thin-film approach offers a new pathway for the development of ultra-compact and ultra-wideband imagers. Wang *et al.* achieved simultaneous encoding of spectral and polarization information by utilizing the nonlocal dispersion characteristics of optically active materials^[165]. Bian *et al.* fabricated a broadband multispectral filter array (BMSFA) mask using photolithography, with different broadband spectral modulation materials distributed at distinct spatial locations^[137]. This mask is integrated into a monochrome image sensor and is capable of encoding high-dimensional hyperspectral information into single-shot measurements. Additionally, they developed a lightweight yet high-performance neural network to reconstruct hyperspectral images from each frame with high fidelity and efficiency. Extensive experiments demonstrated the superiority of the developed hyperspectral imaging sensor over conventional hyperspectral cameras in terms of high spatial-spectral resolution, wide spectral response range, and real-time imaging. Wu *et al.* bonded a vibrating coded microlens array onto a conventional complementary metal-oxide semiconductor (CMOS) sensor to improve spatial sampling density, achieving high-speed aberration-corrected 3D photography

[Fig. 7(a)]^[164]. Tian *et al.* integrated an electrochromic filter array on top of a CMOS sensor and increased the sampling number by tuning the transmission spectra [Fig. 7(c)]^[138]. This technology allows for improving spectral resolution without increasing the number of filters. They also mentioned the potential use of other electrochromic materials, as well as photochromic, force-chromic, and thermochromic materials, to achieve spectral modulation. He *et al.* integrated an optical spacer into a photomultiplier-type organic photodetector (PM-OPD) to achieve electrically tunable spectral response, enabling the capture of the incident spectrum through photocurrent measurement and computational reconstruction using a single device^[166]. Zuo *et al.* achieved single-shot full-Stokes polarization imaging by integrating an ultrathin metasurface polarization filter array onto a visible light imaging sensor [Fig. 7(b)]^[88]. Tang *et al.* modulated the wavelength and polarization resonances of the moiré photonic crystal sensor by changing the interlayer distance and twist angle using integrated MEMS actuators, enabling both hyperspectral and hyperpolarimetric imaging in a single sensor^[167].

Compared with modular optical systems, the integrated systems exhibit reduced configurability and tunability, limiting their adaptability to different tasks or application scenarios. Moreover, micro-nano structures exhibit high susceptibility to environmental variations such as temperature, humidity, and mechanical disturbances, with even slight deformations resulting in significant degradation of optical performance. Nevertheless, innovative computational algorithms promise to alleviate these challenges and lead to performance improvement. Owing to their compactness, lightweight structure, and low power consumption, these imaging systems are particularly suitable for deployment on resource-constrained platforms such as drones and portable instruments. This trend is likely to shape the future of optical modulation, facilitating the widespread application of computational imaging.

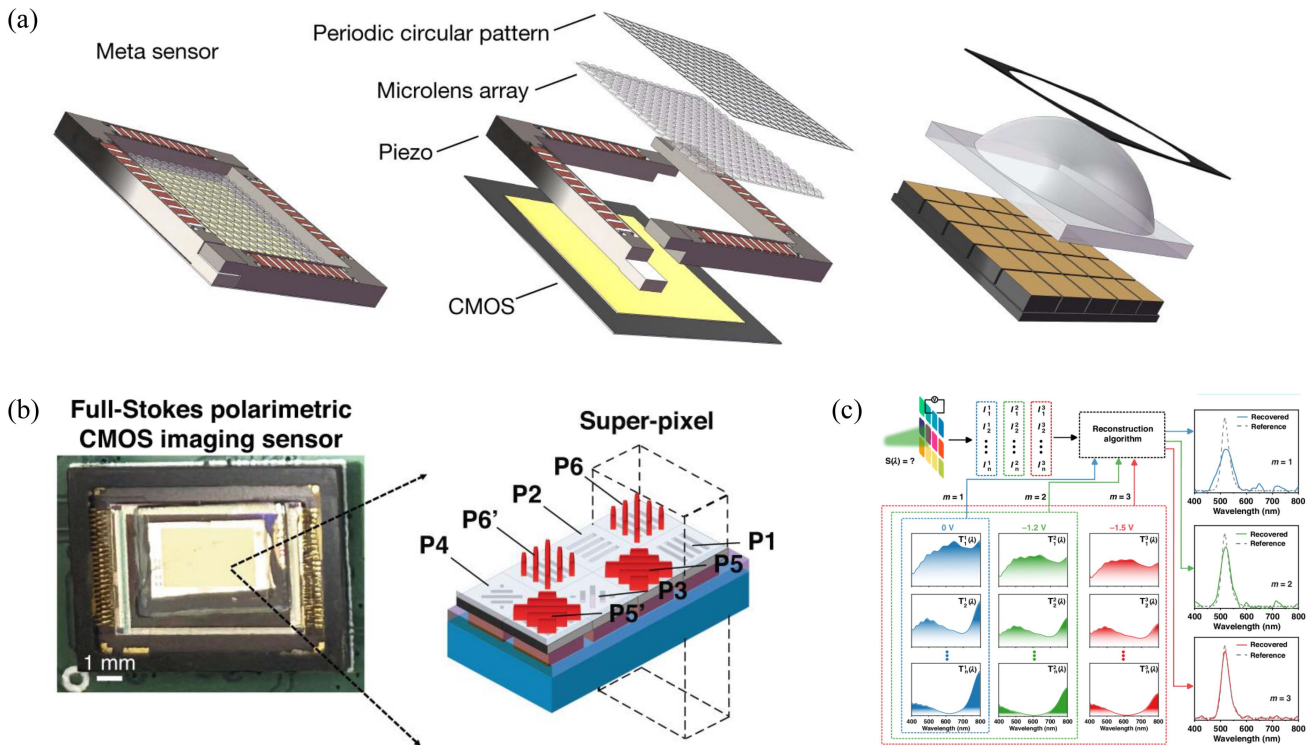


Fig. 7 Integrated and compact optical modulation systems. (a) The meta-imaging sensor (meta sensor) integrates four main elements, reproduced with permission from Springer Nature^[164]. (b) Image of full Stokes polarimetric CMOS imaging sensor, reproduced with permission from Springer Nature^[88]. (c) Principle of the electrochromic computational on-chip spectrometer, reproduced with permission from Springer Nature^[138].

3.2.2. Bio-inspired imaging

Bio-inspired imaging is an artificial imaging technology that imitates the structures and functionalities of biological vision systems. By drawing inspiration from biological eyes in nature, researchers develop imaging systems with unique properties to address issues present in conventional imaging.

In the natural world, many animals have visual systems with unique structures and functionalities that allow them to adapt to the survival demands of different environments. Choi *et al.* thoroughly discussed the research of developing a variety of electronic eyes by mimicking key components and underlying optical principles of natural visual systems^[168]. These electronic eyes incorporate innovative optical elements, such as changeable aperture, hemispherical image sensors, and artificial light reflectors, which enable features like wide-angle viewing, high resolution, and high sensitivity under low-light conditions. Figure 8 shows several recent breakthroughs in bio-inspired imaging. By referring to the structures of animal eyes, Hong *et al.* designed lightguide arrays with multiple shapes and manufactured them using 3D printing technology, achieving high spatial resolution and high spectral resolution imaging [Fig. 8(a)]^[169]. Majorel *et al.* mimicked the optical functionalities of dragonfly compound eyes by integrating directional metalens arrays on a planar surface, achieving 3D imaging with wide FoV and high directional selectivity [Fig. 8(b)]^[170]. This approach overcomes the challenges of optical distortion and manufacturing complexity associated with conventional curved microlens arrays

inspired by insect eyes. Pan *et al.* introduced a novel organic single-crystal phototransistor that features adaptive polarization response [Fig. 8(c)]^[171]. This device can mimic the polarization perception behavior of nocturnal insects under low-light conditions, providing new insights for the development of high-performance polarization detectors and bionic vision systems. Chen *et al.* introduced a bio-inspired CMOS imaging sensor enhanced by vertically stacked photodiodes and perovskite nanocrystals, enabling wavelength-resolved imaging in the ultraviolet spectral range [Fig. 8(d)]^[172]. This design was inspired by the visual system of *Papilio xuthus*, which can detect subtle changes in the ultraviolet spectrum. This sensor has potential applications in medical imaging, military target tracking, remote sensing, and industrial automation.

New materials and micro-nano fabrication technologies have played a crucial role in advancing the development of bio-inspired imaging systems. Empowered by AI, the convergence of bio-inspired computational imaging and neuromorphic vision sensors is expected to achieve breakthroughs in high-speed and energy-efficient imaging, creating new opportunities for many applications.

3.3. Coding on Unconventional Light Properties

Quantum imaging, by harnessing the quantum properties of light such as squeezed light, entangled two-photon states, undetected photons, and single-photon states, promises to surpass

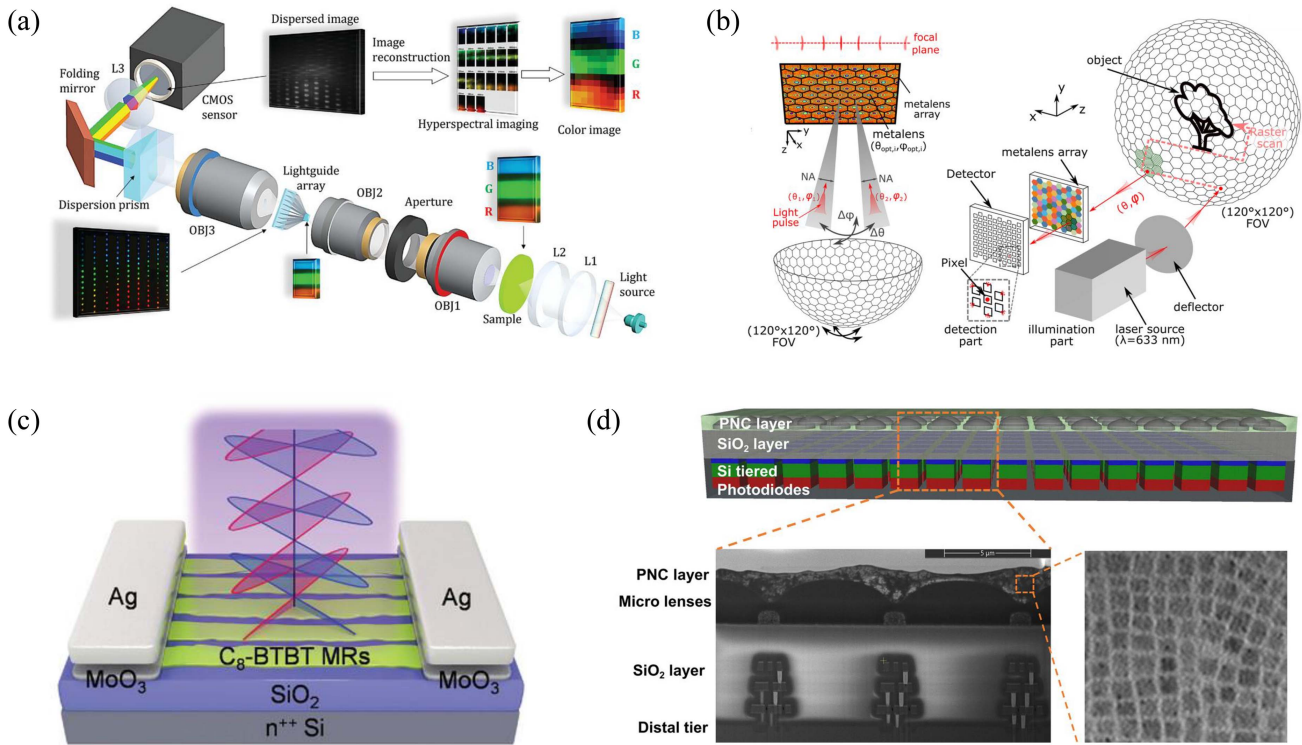


Fig. 8 Bio-inspired imaging systems. (a) Experimental setup for evaluating the performance of the proposed high-resolution snapshot hyperspectral imaging system, reproduced with permission from John Wiley & Sons^[169]. (b) Schematic representation of the metalens array detector and the LiDAR scanning device, reproduced with permission from Springer Nature^[170]. (c) Schematic illustration of the device structure of the polarization-sensitive organic phototransistor (POL-OPT), reproduced with permission from John Wiley & Sons^[171]. (d) Block diagram showing the perovskite nanocrystal (PNC) layer and vertically stacked photodiodes. Images of the PNC-coated sensor and 13 nm cubic PNCs, reproduced with permission from AAAS^[172].

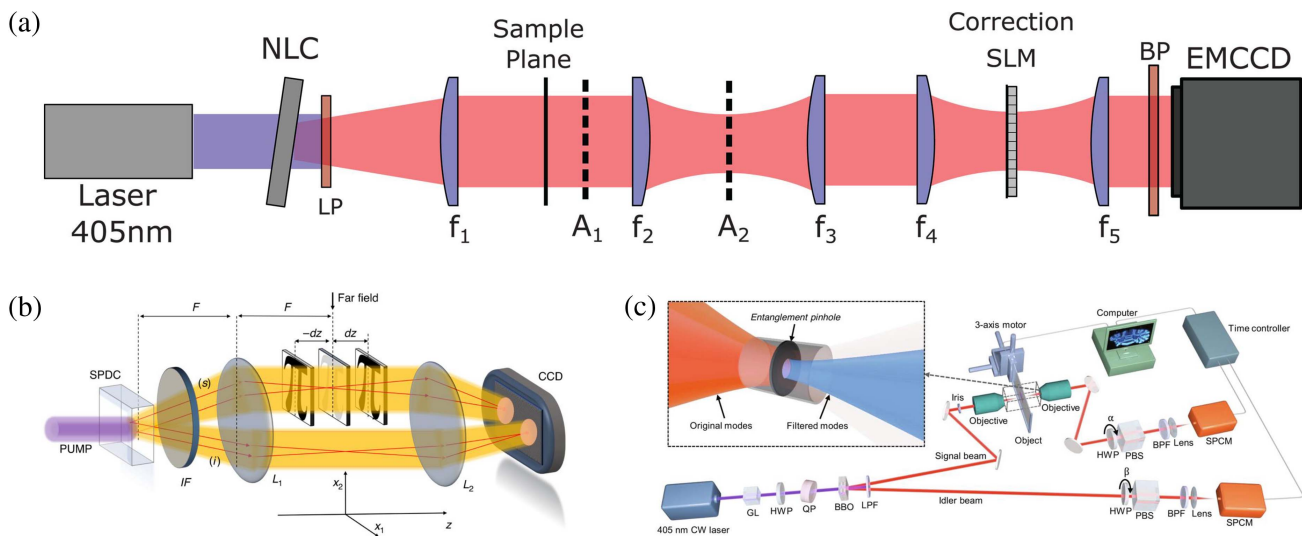


Fig. 9 Quantum imaging systems. (a) Experimental setup for adaptive optical imaging with entangled photons, reproduced with permission from AAAS^[173]. (b) Schematic of non-interferometric quantum-enhanced phase-imaging, reproduced with permission from Springer Nature^[176]. (c) Experimental setup schematics for quantum imaging of biological organisms through spatial and polarization entanglement, reproduced with permission from AAAS^[177].

the fundamental physical limits of classical optics, improving resolution and sensitivity, reducing background noise, and delivering exciting new possibilities^[41]. As shown in Fig. 9, the combination of quantum imaging and computational methods has led to notable advances, further unlocking the potential of quantum imaging in various applications.

Cameron *et al.* proposed quantum-assisted adaptive optics that utilizes the spatial correlations of entangled photon pairs to directly correct the PSF of the imaging system [Fig. 9(a)]^[173]. Experiments showed that it performs better than conventional adaptive optics methods in correcting specific aberrations. Zhang *et al.* proposed quantum correlation hyperspectral imaging that leverages the inherent spectral–temporal correlations of entangled photons to obtain spectral information from the partner photons^[174]. This technique enables the acquisition of spectral information without compromising spatial resolution, and all photons participate in the imaging process, thereby improving the efficiency of resource utilization. Pitsch *et al.* used a single-photon avalanche diode (SPAD) detector array to directly measure the temporal and spatial information of single photons, and they matched entangled photon pairs through time-stamp comparison, achieving 3D quantum ghost imaging^[175]. Ortolano *et al.* conducted experiments using signal and idler photon pairs generated by the spontaneous down-conversion process (SPDC), with the signal photons used to probe the target and the idler photons serving as a noise reference [Fig. 9(b)]^[176]. They measured the intensity at two different positions and achieved non-interferometric QPI based on the transport of intensity equation (TIE). Zhang *et al.* proposed quantum imaging by coincidence from entanglement that leverages spatial entanglement to enhance the SNR and increase the number of resolvable pixels [Fig. 9(c)]^[177]. Additionally, through polarization entanglement, this method enables the remote and instantaneous quantification of the principal refractive index axis angle of an object. Mavian *et al.* achieved high-resolution and high-contrast quantum ghost imaging at extremely low light levels using a single-photon-sensitive time-stamping camera^[178]. Currently, quantum imaging still faces several challenges, including high experimental complexity, low detection efficiency, and high cost. Most techniques remain at the laboratory research stage and lack engineering practicality.

When light propagates with a helical phase wavefront, it has orbital angular momentum (OAM). OAM provides a new degree of freedom of light and has been utilized in optical communication, photonic computing, and optical imaging^[179]. Recent research has demonstrated that OAM possesses distinct advantages for information encoding and improving imaging performance in interferometry, holography, SPI, and microscopy^[179–181]. With the advancement of modulation technology, OAM is set to play an increasingly significant role in imaging applications.

4. Summary and Prospect

Computational imaging leverages the joint design of optical encoding and computational decoding to overcome the physical limits of conventional imaging, thereby improving imaging performance and enabling new functionalities. Information-theoretic analysis of imaging model and advances in optical modulation technology have led to the development of diverse optical encoding methods. Driven by deep learning, differentiable optics and end-to-end optimization enable precise modeling of complex imaging processes and automated optimization

of optical element parameters. Advances in material science and fabrication techniques accelerate the development of integrated, miniaturized, and high-performance imaging systems. Moreover, the non-classical properties of light introduce new degrees of freedom for imaging and demonstrate distinct advantages in specific applications. These encoding methods have gained widespread attention, found diverse applications, and shown great potential for further research.

In nature, animal visual systems have evolved a wide array of structures and functionalities in different environments to meet survival needs. The diverse optical encoding methods make it possible to design and implement specialized cameras for visual tasks in a wide range of application scenarios, including robotics, medical diagnosis, and industrial automation. Future imaging systems tend to transmit the most relevant information for a given task rather than capture full images, which can significantly enhance speed, energy efficiency, and interpretability. Neuromorphic vision sensors emulate the functionality of the human retina and achieve highly efficient visual information processing by responding to changes in pixel intensity. The convergence of computational imaging and neuromorphic cameras holds promise for breakthroughs in ultra-low latency and low-power imaging, as well as improving imaging performance under challenging lighting or weather conditions.

In addition, computational imaging has demonstrated great potential in scientific discoveries. For example, scientists leveraged a global network of radio telescopes and image reconstruction algorithms to capture the first image of a black hole. Future scientific imaging will draw inspiration from embodied AI and will intelligently and dynamically optimize encoding methods based on the interpretation of physical phenomena. This paradigm can enhance the immediate response ability of the imaging systems to weak and transient signals, promising to facilitate the research in dynamic biological processes and extreme physical phenomena.

References

1. J. Liu *et al.*, “Future-proof imaging: computational imaging,” *Adv. Imaging* **1**, 012001 (2024).
2. J. N. Mait, G. W. Euliss, and R. A. Athale, “Computational imaging,” *Adv. Opt. Photonics* **10**, 409 (2018).
3. M. Xiang *et al.*, “Computational optical imaging: challenges, opportunities, new trends, and emerging applications,” *Front. Imaging* **3**, 1336829 (2024).
4. W. T. Cathey *et al.*, “Image gathering and processing for enhanced resolution,” *J. Opt. Soc. Am. A* **1**, 241 (1984).
5. J. N. Mait, R. Athale, and J. van der Gracht, “Evolutionary paths in imaging and recent trends,” *Opt. Express* **11**, 2093 (2003).
6. X. Hu *et al.*, “Metasurface-based computational imaging: a review,” *Adv. Photonics* **6**, 014002 (2024).
7. A. I. Kuznetsov *et al.*, “Roadmap for optical metasurfaces,” *ACS Photonics* **11**, 816 (2024).
8. A. Rhisheekesan *et al.*, “Review on digital holography techniques using digital micromirror device,” *Opt. Lasers Eng.* **177**, 108120 (2024).
9. Y. Yang, A. Forbes, and L. Cao, “A review of liquid crystal spatial light modulators: devices and applications,” *Opto-Electron. Sci.* **2**, 230026 (2023).
10. S. N. Khonina, N. L. Kazanskiy, and M. A. Butt, “Exploring diffractive optical elements and their potential in free space optics and imaging- a comprehensive review,” *Laser Photonics Rev.* **18**, 2400377 (2024).
11. Q. Zhang *et al.*, “Diffractive optical elements 75 years on: from micro-optics to metasurfaces,” *Photonics Insights* **2**, R09 (2023).

12. Y. Guo *et al.*, "Adaptive optics based on machine learning: a review," *Opto-Electron. Adv.* **5**, 200082 (2022).
13. R. Lukac and K. N. Plataniotis, "Color filter arrays: design and performance analysis," *IEEE Trans. Consum. Electron.* **51**, 1260 (2005).
14. X. Li *et al.*, "Polarization 3D imaging technology: a review," *Front. Physics* **11**, 18 (2023).
15. A. Aminzadeh *et al.*, "Mask design, fabrication, and experimental ghost imaging applications for patterned X-ray illumination," *Opt. Express* **31**, 24328 (2023).
16. H. Arguello *et al.*, "Deep optical coding design in computational imaging: a data-driven framework," *IEEE Signal Process. Mag.* **40**, 75 (2023).
17. N. Chen *et al.*, "Differentiable imaging: a new tool for computational optical imaging," *Adv. Phys. Res.* **2**, 2200118 (2023).
18. Z. Wang *et al.*, "Computational optical imaging: on the convergence of physical and digital layers," *Optica* **12**, 113 (2025).
19. X. Yuan, D. J. Brady, and A. K. Katsaggelos, "Snapshot compressive imaging: theory, algorithms, and applications," *IEEE Signal Process. Mag.* **38**, 65 (2021).
20. G. Zheng *et al.*, "Concept, implementations and applications of Fourier ptychography," *Nat. Rev. Phys.* **3**, 207 (2021).
21. M. Bertero, P. Boccacci, and A. K. De Mol, *Introduction to Inverse Problems in Imaging*, CRC Press (2021).
22. S. Boyd *et al.*, "Distributed optimization and statistical learning via the alternating direction method of multipliers," *Found. Trends Mach. LEARN.* **3**, 1 (2011).
23. P. Blomgren and T. F. Chan, "Color TV: total variation methods for restoration of vector-valued images," *IEEE Trans. Image Process.* **7**, 304 (1998).
24. Y. Gao and L. Cao, "Iterative projection meets sparsity regularization: towards practical single-shot quantitative phase imaging with in-line holography," *Light-Adv. Manuf.* **4**, 37 (2023).
25. G. Barbastathis, A. Ozcan, and G. Situ, "On the use of deep learning for computational imaging," *Optica* **6**, 921 (2019).
26. K. Wang *et al.*, "On the use of deep learning for phase recovery," *Light-Sci. Appl.* **13**, 4 (2024).
27. C. Banerjee *et al.*, "Physics-informed computer vision: a review and perspectives," *ACM Comput. Surv.* **57**, 38 (2024).
28. Z. Wu *et al.*, "Latent diffusion prior enhanced deep unfolding for snapshot spectral compressive imaging," in *European Conference on Computer Vision (ECCV)* (2025), p. 164.
29. U. S. Kamilov *et al.*, "Plug-and-play methods for integrating physical and learned models in computational imaging: theory, algorithms, and applications," *IEEE Signal Process. Mag.* **40**, 85 (2023).
30. G. Wu *et al.*, "Light field image processing: an overview," *IEEE J. Sel. Top. Signal Process.* **11**, 926 (2017).
31. J. Geng, "Structured-light 3D surface imaging: a tutorial," *Adv. Opt. Photonics* **3**, 128 (2011).
32. P. C. Chaumet *et al.*, "Quantitative phase microscopies: accuracy comparison," *Light-Sci. Appl.* **13**, 288 (2024).
33. D. Faccio, A. Velten, and G. Wetzstein, "Non-line-of-sight imaging," *Nat. Rev. Phys.* **2**, 318 (2020).
34. Z. Yu *et al.*, "Wavefront shaping: a versatile tool to conquer multiple scattering in multidisciplinary fields," *The Innovation* **3**, 100292 (2022).
35. M. P. Edgar, G. M. Gibson, and M. J. Padgett, "Principles and prospects for single-pixel imaging," *Nat. Photonics* **13**, 13 (2019).
36. P. J. Withers *et al.*, "X-ray computed tomography," *Nat. Rev. Methods Primers* **1**, 18 (2021).
37. K. Hammernik *et al.*, "Physics-driven deep learning for computational magnetic resonance imaging: combining physics and machine learning for improved medical imaging," *IEEE Signal Process. Mag.* **40**, 98 (2023).
38. D. J. Brady *et al.*, "Compressive holography," *Opt. Express* **17**, 13040 (2009).
39. D. J. Brady *et al.*, "Compressive tomography," *Adv. Opt. Photonics* **7**, 756 (2015).
40. M. Qiao *et al.*, "Snapshot coherence tomographic imaging," *IEEE Trans. Comput. Imaging* **7**, 624 (2021).
41. H. Defienne *et al.*, "Advances in quantum imaging," *Nat. Photonics* **18**, 1024 (2024).
42. F. O. Huck, C. L. Fales, and Z.-U. Rahman, "An information theory of visual communication," *Philos. Trans. R. Soc. London A* **354**, 2193 (1997).
43. X. Zhang *et al.*, "Different channels to transmit information in scattering media," *Photonix* **4**, 10 (2023).
44. J. Bertolotti and O. Katz, "Imaging in complex media," *Nat. Physics* **18**, 1008 (2022).
45. Z. Wang *et al.*, "Coded self-referencing wavefront shaping for fast dynamic scattering control," *Adv. Imaging* **2**, 011002 (2025).
46. C. Zuo *et al.*, "Temporal phase unwrapping algorithms for fringe projection profilometry: a comparative review," *Opt. Lasers Eng.* **85**, 84 (2016).
47. J. Deng *et al.*, "Robust phase-coding: a solution to suppress fringe order errors," *Opt. Express* **32**, 36742 (2024).
48. Z. Sun *et al.*, "Robust structured light with efficient redundant codes," *Opt. Express* **32**, 33507 (2024).
49. X. Li *et al.*, "Three-dimensional structured illumination microscopy with enhanced axial resolution," *Nat. Biotechnol.* **41**, 1307 (2023).
50. A. G. York *et al.*, "Resolution doubling in live, multicellular organisms via multifocal structured illumination microscopy," *Nat. Methods* **9**, 749 (2012).
51. Ø. I. Helle *et al.*, "Structured illumination microscopy using a photonic chip," *Nat. Photonics* **14**, 431 (2020).
52. M. T. M. Hannebelle *et al.*, "Open-source microscope add-on for structured illumination microscopy," *Nat. Commun.* **15**, 1550 (2024).
53. O. Barlev and M. A. Golub, "Multifunctional binary diffractive optical elements for structured light projectors," *Opt. Express* **26**, 21092 (2018).
54. D. Dan *et al.*, "DMD-based LED-illumination super-resolution and optical sectioning microscopy," *Sci. Rep.* **3**, 1116 (2013).
55. G. Kim *et al.*, "Metasurface-driven full-space structured light for three-dimensional imaging," *Nat. Commun.* **13**, 5920 (2022).
56. G. Zheng, R. Horstmeyer, and C. Yang, "Wide-field, high-resolution Fourier ptychographic microscopy," *Nat. Photonics* **7**, 739 (2013).
57. L. Bian *et al.*, "Content adaptive illumination for Fourier ptychography," *Opt. Lett.* **39**, 6648 (2014).
58. Y. Zhang *et al.*, "Self-learning based Fourier ptychographic microscopy," *Opt. Express* **23**, 18471 (2015).
59. J. Sun *et al.*, "Single-shot quantitative phase microscopy based on color-multiplexed Fourier ptychography," *Opt. Lett.* **43**, 3365 (2018).
60. L. Tian *et al.*, "Multiplexed coded illumination for Fourier ptychography with an LED array microscope," *Biomed. Opt. Express* **5**, 2376 (2014).
61. S. Dong *et al.*, "Spectral multiplexing and coherent-state decomposition in Fourier ptychographic imaging," *Biomed. Opt. Express* **5**, 1757 (2014).
62. Y. Zhou *et al.*, "Fourier ptychographic microscopy using wavelength multiplexing," *J. Biomed. Opt.* **22**, 066006 (2017).
63. L. Tian *et al.*, "Computational illumination for high-speed *in vitro* Fourier ptychographic microscopy," *Optica* **2**, 904 (2015).
64. X. Wu *et al.*, "Lens-free on-chip 3D microscopy based on wavelength-scanning Fourier ptychographic diffraction tomography," *Light-Sci. Appl.* **13**, 237 (2024).
65. C. Kuang *et al.*, "Digital micromirror device-based laser-illumination Fourier ptychographic microscopy," *Opt. Express* **23**, 26999 (2015).

66. J. Chung *et al.*, "Wide-field Fourier ptychographic microscopy using laser illumination source," *Biomed. Opt. Express* **7**, 4787 (2016).
67. X. Tao *et al.*, "Tunable-illumination for laser Fourier ptychographic microscopy based on a background noise-reducing system," *Opt. Commun.* **468**, 125764 (2020).
68. I. Coddington *et al.*, "Rapid and precise absolute distance measurements at long range," *Nat. Photonics* **3**, 351 (2009).
69. A. D. Payne *et al.*, "Improved measurement linearity and precision for AMCW time-of-flight range imaging cameras," *Appl. Opt.* **49**, 4392 (2010).
70. D. J. Lum, S. H. Knarr, and J. C. Howell, "Frequency-modulated continuous-wave LiDAR compressive depth-mapping," *Opt. Express* **26**, 15420 (2018).
71. M. L. Simpson *et al.*, "Intensity-modulated, stepped frequency cw lidar for distributed aerosol and hard target measurements," *Appl. Opt.* **44**, 7210 (2005).
72. N. Li *et al.*, "Spectral imaging and spectral LIDAR systems: moving toward compact nanophotonics-based sensing," *Nanophotonics* **10**, 1437 (2021).
73. Y. Jiang, S. Karpf, and B. Jalali, "Time-stretch LiDAR as a spectrally scanned time-of-flight ranging camera," *Nat. Photonics* **14**, 14 (2020).
74. R. Juliano Matins *et al.*, "Metasurface-enhanced light detection and ranging technology," *Nat. Commun.* **13**, 5724 (2022).
75. R. Raskar, A. Agrawal, and J. Tumblin, "Coded exposure photography: motion deblurring using fluttered shutter," *ACM Trans. Graph.* **25**, 795 (2006).
76. H.-G. Jeon *et al.*, "Generating fluttering patterns with low auto-correlation for coded exposure imaging," *International Journal of Computer Vision* **123**, 269 (2017).
77. Y. Hitomi *et al.*, "Video from a single coded exposure photograph using a learned over-complete dictionary," in *IEEE International Conference on Computer Vision (ICCV)* (2011), p. 287.
78. J. Zhang *et al.*, "Pixel-wise programmability enables dynamic high-SNR cameras for high-speed microscopy," *Nat. Commun.* **15**, 4480 (2024).
79. Y. Luo *et al.*, "CMOS computational camera with a two-tap coded exposure image sensor for single-shot spatial-temporal compressive sensing," *Opt. Express* **27**, 31475 (2019).
80. D. Huang *et al.*, "Optical coherence tomography," *Science* **254**, 1178 (1991).
81. A. F. Fercher *et al.*, "Measurement of intraocular distances by backscattering spectral interferometry," *Opt. Commun.* **117**, 43 (1995).
82. S. R. Chinn, E. A. Swanson, and J. G. Fujimoto, "Optical coherence tomography using a frequency-tunable optical source," *Opt. Lett.* **22**, 340 (1997).
83. I. Yamaguchi and T. Zhang, "Phase-shifting digital holography," *Opt. Lett.* **22**, 1268 (1997).
84. E. Sánchez-Ortiga *et al.*, "Off-axis digital holographic microscopy: practical design parameters for operating at diffraction limit," *Appl. Opt.* **53**, 2058 (2014).
85. F. Wang *et al.*, "Visible achromatic metalens design based on artificial neural network," *Adv. Opt. Mater.* **10**, 2101842 (2022).
86. J. Seo *et al.*, "Deep-learning-driven end-to-end metalens imaging," *Adv. Photonics* **6**, 066002 (2024).
87. C.-H. Lin *et al.*, "Metasurface-empowered snapshot hyperspectral imaging with convex/deep (CODE) small-data learning theory," *Nat. Commun.* **14**, 6979 (2023).
88. J. Zuo *et al.*, "Chip-integrated metasurface full-Stokes polarimetric imaging sensor," *Light-Sci. Appl.* **12**, 218 (2023).
89. X. Wu *et al.*, "Wavelength-insensitive snapshot Stokes polarimetric imaging based on cascaded metasurfaces," *Adv. Photonics* **7**, 016008 (2025).
90. A. Zaidi *et al.*, "Metasurface-enabled single-shot and complete Mueller matrix imaging," *Nat. Photonics* **18**, 704 (2024).
91. N. A. Rubin *et al.*, "Matrix Fourier optics enables a compact full-Stokes polarization camera," *Science* **365**, eaax1839 (2019).
92. W. Liu *et al.*, "Aberration-corrected three-dimensional positioning with a single-shot metalens array," *Optica* **7**, 1706 (2020).
93. F. Zhao *et al.*, "Synthetic aperture metalens," *Photonics Res.* **9**, 2388 (2021).
94. Z. Lin *et al.*, "End-to-end metasurface inverse design for single-shot multi-channel imaging," *Opt. Express* **30**, 28358 (2022).
95. B. Wilburn *et al.*, "High performance imaging using large camera arrays," *ACM Trans. Graph.* **24**, 765 (2005).
96. S. Zhu, J. Sasián, and D. J. Brady, "Multifocal array camera system design," *Appl. Opt.* **63**, 6553 (2024).
97. N. Genser, J. Seiler, and A. Kaup, "Camera array for multi-spectral imaging," *IEEE Trans. Image Process.* **29**, 9234 (2020).
98. A. C. S. Chan *et al.*, "Parallel Fourier ptychographic microscopy for high-throughput screening with 96 cameras (96 Eyes)," *Sci. Rep.* **9**, 11114 (2019).
99. J. Kopf *et al.*, "Capturing and viewing gigapixel images," *ACM Trans. Graph.* **26**, 10 (2007).
100. T. Skauli *et al.*, "Compact camera for multispectral and conventional imaging based on patterned filters," *Appl. Opt.* **53**, C64 (2014).
101. J. Holloway *et al.*, "SAVI: synthetic apertures for long-range, subdiffraction-limited visible imaging using Fourier ptychography," *Sci. Adv.* **3**, e1602564 (2017).
102. R. H. Dicke, "Scatter-hole cameras for x-rays and gamma rays," *Astrophys. J.* **153**, L101 (1968).
103. E. E. Fenimore and T. M. Cannon, "Coded aperture imaging with uniformly redundant arrays," *Appl. Opt.* **17**, 337 (1978).
104. S. R. Gottesman and E. E. Fenimore, "New family of binary arrays for coded aperture imaging," *Appl. Opt.* **28**, 4344 (1989).
105. J. Wu *et al.*, "Single-shot lensless imaging with Fresnel zone aperture and incoherent illumination," *Light-Sci. Appl.* **9**, 53 (2020).
106. E. Vargas, H. Rueda-Chacón, and H. Arguello, "Learning time-multiplexed phase-coded apertures for snapshot spectral-depth imaging," *Opt. Express* **31**, 39796 (2023).
107. T. Luo, L. Wang, and X. Yuan, "Grating-based coded aperture compressive spectral imaging to reconstruct over 190 spectral bands from a snapshot measurement," *J. Phys. D-Appl. Phys.* **56**, 254004 (2023).
108. F. Heide *et al.*, "High-quality computational imaging through simple lenses," *ACM Trans. Graph.* **32**, 14 (2013).
109. K. Kubala, E. Dowski, and W. T. Cathey, "Reducing complexity in computational imaging systems," *Opt. Express* **11**, 2102 (2003).
110. V. Boominathan *et al.*, "Recent advances in lensless imaging," *Optica* **9**, 1 (2022).
111. X. Dun *et al.*, "Learned rotationally symmetric diffractive achromat for full-spectrum computational imaging," *Optica* **7**, 913 (2020).
112. V. Akondi and A. Dubra, "Multi-layer Shack-Hartmann wavefront sensing in the point source regime," *Biomed. Opt. Express* **12**, 409 (2021).
113. F. Roddier, "Curvature sensing and compensation: a new concept in adaptive optics," *Appl. Opt.* **27**, 1223 (1988).
114. I. Iglesias, "Pyramid phase microscopy," *Opt. Lett.* **36**, 3636 (2011).
115. T. Wu *et al.*, "Multiplexed wavefront sensing with a thin diffruser," *Optica* **11**, 297 (2024).
116. K. M. Hampson *et al.*, "Adaptive optics for high-resolution imaging," *Nat. Rev. Methods Primers* **1**, 68 (2021).
117. D. Bergmann, "New approach for automatic surface reconstruction with coded light," in *Remote Sensing and Reconstruction for Three-Dimensional Objects and Scenes* (1995), p. 2.

118. L. Hu *et al.*, “Phase-only liquid-crystal spatial light modulator for wave-front correction with high precision,” *Opt. Express* **12**, 6403 (2004).
119. P. Rajaeipour *et al.*, “Cascading optofluidic phase modulators for performance enhancement in refractive adaptive optics,” *Adv. Photonics* **2**, 066005 (2020).
120. A. Lumsdaine and T. Georgiev, “The focused plenoptic camera,” in *IEEE International Conference on Computational Photography (ICCP)* (2009), p. 1.
121. L.-L. Ma *et al.*, “Self-assembled asymmetric microlenses for four-dimensional visual imaging,” *ACS Nano* **13**, 13709 (2019).
122. C. Yu *et al.*, “Microlens array snapshot hyperspectral microscopy system for the biomedical domain,” *Appl. Opt.* **60**, 1896 (2021).
123. K. Song *et al.*, “Advances and challenges of single-pixel imaging based on deep learning,” *Laser Photonics Rev.* **19**, 2401397.
124. A. Paniate *et al.*, “Light-field ghost imaging,” *Phys. Rev. Appl.* **21**, 024032 (2024).
125. Z.-P. Li *et al.*, “Single-photon imaging over 200 km,” *Optica* **8**, 344 (2021).
126. X. F. Zhang *et al.*, “Super-resolution imaging for infrared micro-scanning optical system,” *Opt. Express* **27**, 7719 (2019).
127. L.-L. Xiao *et al.*, “A compressed sensing approach for enhancing infrared imaging resolution,” *Opt. Laser Technol.* **44**, 2354 (2012).
128. F. Yang *et al.*, “A four-aperture super-resolution camera based on adaptive regularization parameter tuning,” *Opt. Lasers Eng.* **165**, 107562 (2023).
129. Z. Wang *et al.*, “Adaptive high-resolution imaging method based on compressive sensing,” *Sensors* **22**, 8848 (2022).
130. Z. Xia *et al.*, “A novel space-borne high-resolution SAR system with the non-uniform hybrid sampling technology for space targets imaging,” *Appl. Sci.-Basel* **12**, 4848 (2022).
131. A. Gao *et al.*, “Real-time stereo 3D car detection with shape-aware non-uniform sampling,” *IEEE Trans. Intell. Transp. Syst.* **24**, 4027 (2023).
132. A. J. J. M. van Breemen *et al.*, “Curved digital X-ray detectors,” *npj Flexible Electronics* **4**, 22 (2020).
133. L. Gu *et al.*, “A biomimetic eye with a hemispherical perovskite nanowire array retina,” *Nature* **581**, 278 (2020).
134. Z. Rao *et al.*, “Curvy, shape-adaptive imagers based on printed optoelectronic pixels with a kirigami design,” *Nat. Electronics* **4**, 513 (2021).
135. X. Yu *et al.*, “Multispectral curved compound eye camera,” *Opt. Express* **28**, 9216 (2020).
136. Y. Fan *et al.*, “Dispersion-assisted high-dimensional photodetector,” *Nature* **630**, 77 (2024).
137. L. Bian *et al.*, “A broadband hyperspectral image sensor with high spatio-temporal resolution,” *Nature* **635**, 73 (2024).
138. M. Tian *et al.*, “Miniaturized on-chip spectrometer enabled by electrochromic modulation,” *Light-Sci. Appl.* **13**, 278 (2024).
139. F. Feng *et al.*, “Symbiotic evolution of photonics and artificial intelligence: a comprehensive review,” *Adv. Photonics* **7**, 78 (2025).
140. C. Y. Shen *et al.*, “Broadband unidirectional visible imaging using wafer-scale nano-fabrication of multi-layer diffractive optical processors,” *Light-Sci. Appl.* **14**, 18 (2025).
141. O. Kulce *et al.*, “All-optical information-processing capacity of diffractive surfaces,” *Light-Sci. Appl.* **10**, 17 (2021).
142. C. Y. Shen *et al.*, “Multiplane quantitative phase imaging using a wavelength-multiplexed diffractive optical processor,” *Adv. Photonics* **6**, 19 (2024).
143. D. Mengu *et al.*, “Snapshot multispectral imaging using a diffractive optical network,” *Light-Sci. Appl.* **12**, 20 (2023).
144. A. Silva *et al.*, “Performing mathematical operations with metamaterials,” *Science* **343**, 160 (2014).
145. X. Lin *et al.*, “All-optical machine learning using diffractive deep neural networks,” *Science* **361**, 1004 (2018).
146. J. Shi *et al.*, “Rapid all-in-focus imaging via physical neural network optical encoding,” *Opt. Lasers Eng.* **164**, 107520 (2023).
147. J. Hu *et al.*, “Subwavelength imaging using a solid-immersion diffractive optical processor,” *eLight* **4**, 8 (2024).
148. J. Zhao *et al.*, “Real-time anti-turbulence imaging using a diffractive optical processor,” *Opt. Lasers Eng.* **186**, 11 (2025).
149. V. Sitzmann *et al.*, “End-to-end optimization of optics and image processing for achromatic extended depth of field and super-resolution imaging,” *ACM Trans. Graph.* **37**, 1 (2018).
150. L. Desdoigts *et al.*, “Differentiable optics with ∂ Lux: I—deep calibration of flat field and phase retrieval with automatic differentiation,” *J. Astron. Telesc. Instrum. Syst.* **9**, 028007 (2023).
151. J. Bacca, T. Gelvez-Barrera, and H. Arguello, “Deep coded aperture design: an end-to-end approach for computational imaging tasks,” *IEEE Trans. Comput. Imaging* **7**, 1148 (2021).
152. R. Jacome, P. Gomez, and H. Arguello, “Middle output regularized end-to-end optimization for computational imaging,” *Optica* **10**, 1421 (2023).
153. Z. Li *et al.*, “Empowering metasurfaces with inverse design: principles and applications,” *ACS Photonics* **9**, 2178 (2022).
154. L. Zhu *et al.*, “Direct computational ghost imaging via speckle patterns based on multi-social genetic algorithm,” *Opt. Commun.* **579**, 131465 (2025).
155. C. Zheng, G. Zhao, and P. So, “Close the design-to-manufacturing gap in computational optics with a ‘Real2Sim’ learned two-photon neural lithography simulator,” in *SIGGRAPH Asia 2023 Conference Papers* (2023) p. 1.
156. G. Arya *et al.*, “End-to-end optimization of metasurfaces for imaging with compressed sensing,” *ACS Photonics* **11**, 2077 (2024).
157. N. Chen, C. Wang, and W. Heidrich, “ ∂ H: differentiable holography,” *Laser Photonics Rev.* **17**, 2200828 (2023).
158. B. Seong *et al.*, “E2E-BPF microscope: extended depth-of-field microscopy using learning-based implementation of binary phase filter and image deconvolution,” *Light-Sci. Appl.* **12**, 269 (2023).
159. Y. Shao *et al.*, “Wavelength-multiplexed multi-mode EUV reflection ptychography based on automatic differentiation,” *Light-Sci. Appl.* **13**, 196 (2024).
160. J. Wang, K. Li, and Z. Quan, “Integrated structured light manipulation,” *Photonics Insights* **3**, R05 (2024).
161. B. Lyu *et al.*, “Multi-wavelength structured light based on metasurfaces for 3D imaging,” *Nanophotonics* **13**, 477 (2024).
162. C. Lin, Y. Guo, and N. Le Thomas, “Demonstration of a photonic integrated circuit for quantitative phase imaging,” *Photonics Res.* **13**, 1 (2025).
163. I. Kim *et al.*, “Nanophotonics for light detection and ranging technology,” *Nat. Nanotechnol.* **16**, 508 (2021).
164. J. Wu *et al.*, “An integrated imaging sensor for aberration-corrected 3D photography,” *Nature* **612**, 62 (2022).
165. X. Wang *et al.*, “Exploiting universal nonlocal dispersion in optically active materials for spectro-polarimetric computational imaging,” *eLight* **4**, 22 (2024).
166. X. He *et al.*, “A microsized optical spectrometer based on an organic photodetector with an electrically tunable spectral response,” *Nat. Electronics* **7**, 694 (2024).
167. H. Tang *et al.*, “An adaptive moiré sensor for spectro-polarimetric hyperimaging,” *Nat. Photonics* **19**, 463 (2025).
168. C. Choi *et al.*, “Inspiration from visual ecology for advancing multifunctional robotic vision systems: bio-inspired electronic eyes and neuromorphic image sensors,” *Adv. Mater.* **36**, 2412252 (2024).
169. Z. Hong *et al.*, “Bio-inspired compact, high-resolution snapshot hyperspectral imaging system with 3D printed glass lightguide array,” *Adv. Opt. Mater.* **11**, 2300156 (2023).
170. C. Majorel *et al.*, “Bio-inspired flat optics for directional 3D light detection and ranging,” *npj Nanophotonics* **1**, 18 (2024).

171. J. Pan *et al.*, "Self-adaptive polarized photoresponse in organic single-crystal phototransistors for bionic night-time polarization perception," *Adv. Mater.* **37**, 10 (2025).
172. C. Chen *et al.*, "Bioinspired, vertically stacked, and perovskite nanocrystal-enhanced CMOS imaging sensors for resolving UV spectral signatures," *Sci. Adv.* **9**, eadk3860 (2023).
173. P. Cameron *et al.*, "Adaptive optical imaging with entangled photons," *Science* **383**, 1142 (2024).
174. Y. Zhang, D. England, and B. Sussman, "Snapshot hyperspectral imaging with quantum correlated photons," *Opt. Express* **31**, 2282 (2023).
175. C. Pitsch *et al.*, "3D quantum ghost imaging," *Appl. Opt.* **62**, 6275 (2023).
176. G. Ortolano *et al.*, "Quantum enhanced non-interferometric quantitative phase imaging," *Light-Sci. Appl.* **12**, 171 (2023).
177. Y. Zhang *et al.*, "Quantum imaging of biological organisms through spatial and polarization entanglement," *Sci. Adv.* **10**, eadk1495 (2024).
178. A. Mavian *et al.*, "Fast quantum ghost imaging with a single-photon-sensitive time-stamping camera," *Opt. Lett.* **50**, 594 (2025).
179. J. Zeng *et al.*, "Optical imaging using orbital angular momentum: interferometry, holography and microscopy," *J. Lightwave Technol.* **41**, 2025 (2023).
180. H. Ren *et al.*, "Metasurface orbital angular momentum holography," *Nat. Commun.* **10**, 2986 (2019).
181. L. Gao *et al.*, "OAM-basis wavefront single-pixel imaging via compressed sensing," *J. Lightwave Technol.* **41**, 2131 (2023).